Molecular Jamming in Tortuous Nanochannels

Petr Dementyev,[*,†] *Yang Yang,*[*,†,‡] *Maria Rezvova,*[†,§] *Armin Gölzhäuser*[†]

[†]Physics of Supramolecular Systems and Surfaces, Faculty of Physics, Bielefeld University, Bielefeld, 33615 Germany

[‡]Barrer Centre, Imperial College London, London, SW7 2AZ United Kingdom

[§]Research Institute for Complex Issues of Cardiovascular Diseases, Kemerovo, 650002 Russian Federation

Corresponding Authors

*(dementyev@physik.uni-bielefeld.de (P.D.); yang.yang1@imperial.ac.uk (Y.Y.))

ABSTRACT

Ultrathin nanostructured membranes are widely pursued to apply into different processes ranging from air separation to seawater desalination. Here, freestanding carbon nanomembranes (CNMs) are employed to dehydrate vaporous alcohols at room temperature. The structure of the microporous material is addressed by measuring permeation rates of homologous n-alkanols. To examine the separation performance, we introduce a model heavy water/n-propanol azeotrope. While ordinary nanomembranes show a moderate selectivity of around 300, complete rejection of organic molecules is achieved upon stacking two CNM layers. Furthermore, the mixture experiments with the stacks demonstrate a tenfold slowdown in the transmembrane diffusion of water as compared to both the single-layer material and pure vapor. We discuss the observed effect as a “molecular jam” in the interlayer spacing which effectively disrupts the collective flow of liquefied water. Our work sheds light on molecular transport under nanoconfinement.

TOC GRAPHICS

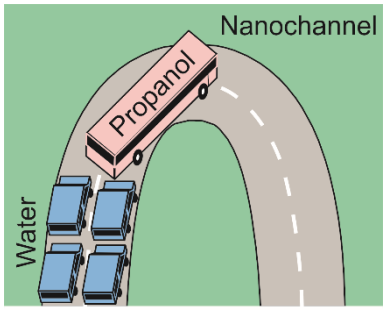

A wider use of bioenergy is considered to be one of the urgent measures to mitigate climate change.[1] The fermentation-based conversion of biomass into small organic molecules, in particular alcohols, is a well-established technological process. However, the production of fuel-grade alcohols requires additional energy-intensive dehydration steps.[2] While fractional distillation is the most universal method, it fails at breaking azeotropic mixtures. In this context, membrane separation offers many potential advantages, such as continuous operation and higher energy efficiency.[3-5] Graphene oxide (GO) and other nanostructured materials have been shown to enable ultrafast permeation of water which is associated with the collective diffusion of hydrogen-bonded molecules.[6-10] Despite the immense potential for selective removal of water, the single-file phenomenon demands further fundamental studies and better mechanistic understanding.[11-15] As to azeotrope separation, the interactions of water and alcohol molecules both with the working material and with each other represent one of the key factors in membrane performance. It was pioneered by Schrier that the mass transfer across porous 2D materials can be described in terms of molecular adsorption on the membrane surface.[16] Recently, Dementyev and co-workers presented vapor permeation measurements revealing the impact of interfacial effects on cross-membrane transport, including water-assisted passage of various species.[17] The new experimental method, henceforth as *Adsorption Controlled Permeation* (ACP), appears to be powerful not only for probing surface phenomena, but also more broadly for studying molecular diffusion in nanomaterials. This paper demonstrates that exposing ultrathin membranes to well-defined feed environments and measuring flow rates yield valuable information on kinetic processes occurring inside the material. More specifically, we report on an unprecedented decrease in the infiltration of water through double-layer carbon nanomembranes (CNMs) upon mixing with 1-propanol (PrOH).

Bottom-up synthesized CNMs of 1 nm in thickness were previously found to pass water vapor through a myriad of sub-nanometer channels as fast as carbon nanotubes (CNTs) and aquaporins.[10] The results agreed with pervaporation measurements, and humidity-dependent condensation was justified to take place on CNMs.[18] The experiments with organic vapors and binary mixtures revealed that surface-mediated permeation is possible for many adsorbing substances, and even inert gases can enter the membrane channels upon dissolving in liquefied water.[17] Herein, suspended nanomembranes of around 7 μm in diameter were exposed to vaporous alcohols $C_nH_{2n+1}OH$ (n=1-4), and steady-state flow rates were measured by means of the original permeation system equipped with a quadrupole mass-spectrometer (QMS).[18] Fig. 1 shows molecular fluxes for the anhydrous compounds under feed conditions corresponding to saturated vapors at room temperature. To a first approximation, the alcohols are chemically similar and entail equivalent amounts of adsorbates on the membrane surface upon saturation. As expected, shorter molecules of methanol (MeOH) and ethanol (EtOH) readily cross ordinary CNMs, whereas the permeation of PrOH and 1-butanol (BuOH) is not observed for the micrometer-sized samples. When two CNMs sheets are stacked together forming van der Waals composites,[19] the permeation rate for MeOH drops down by almost two orders of magnitude, and the flow of EtOH turns out to be below the detection limit. The earlier atomic-force microscopy (AFM) images revealed a sponge-like morphology of CNMs with the pore diameter *d* ranging from 0.4 to 1.0 nm (Fig. 2a).[10] The present study confirms our later suggestion that the membranes are laminar, and the features seen in AFM are only entrances to their tortuous nanochannels.[17] In turn, structural characterization of CNMs with high-resolution electron microcopy is complicated due to beam heating and further conversion to graphene.[20]

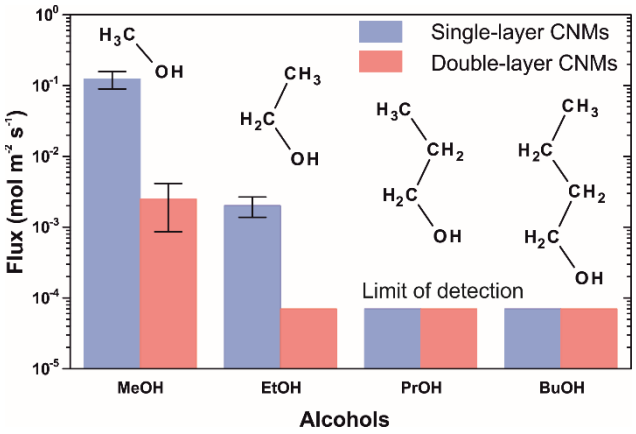

Figure 1. Transmembrane flux of pure alcohols in single- and double-layer CNMs. The following feed pressures were applied: p(MeOH) ≈ 155 mbar (sat.); p(EtOH) ≈ 70 mbar (sat.); p(PrOH) ≈ 26 mbar (sat.); p(BuOH) ≈ 9 mbar (sat.). The data are mean values over 3 samples, and the error bars are standard deviation.

Table 1. Molecular length calculated with the cylinder diameter of 0.29 nm.

Species	Water	MeOH	EtOH	PrOH	BuOH
Length, nm	0.30	0.53	0.79	1.04	1.29

In order to get a sense for the channels dimensions, we simulated 1-alkanol molecules as rod-shaped ones according to Marcus and calculated their effective cylinder lengths *l* based on the van der Waals volumes.[21] The molecular size increases incrementally from MeOH to BuOH, and water molecules appear to be almost globular (Table 1). Based on this crude approximation and neglecting conformational changes of molecules, we devise a simplified geometrical model for CNMs' microstructure (Fig. 2). There are two linear parameters *t* and *h* to account for the channel tortuosity. If the twist $t \leq 0$, the membrane pores would be straight, and permeation of gaseous particles would be observed. For $l \leq d$, flat-lying MeOH and EtOH molecules are expected to reach

the pore hollows, and their further diffusion through the channels is likely to depend on the values of *h* and *t*. As prescribed by the distribution of *d* (Fig. 2a) and the molecular length *l* (Table 1), the probability of the angle α to be 0° amounts to 82% and 31% for MeOH and EtOH, respectively. However, the actual passage rate for the two substances differs by orders of magnitude, indicating that MeOH molecules can enter the channels at various α (Fig. 1). It is also possible that MeOH is engaged in hydrogen bonding and reveals single-file transport similar to water. Given the unimpeded flow of water molecules, the height *h* has the lower limit of at least 0.3 nm, and its higher bound can be set to 0.7 nm as a cutoff for upright standing EtOH molecules (α=90°). As permeation of alcohols in the CNMs stacks changes drastically, their interlayer spacing *s* seems to be the rate-limiting parameter with the narrowest size distribution. Indeed, two-dimensional heterostructures are known to exhibit strong adhesion properties due to their nanoscale flexibility.[22]

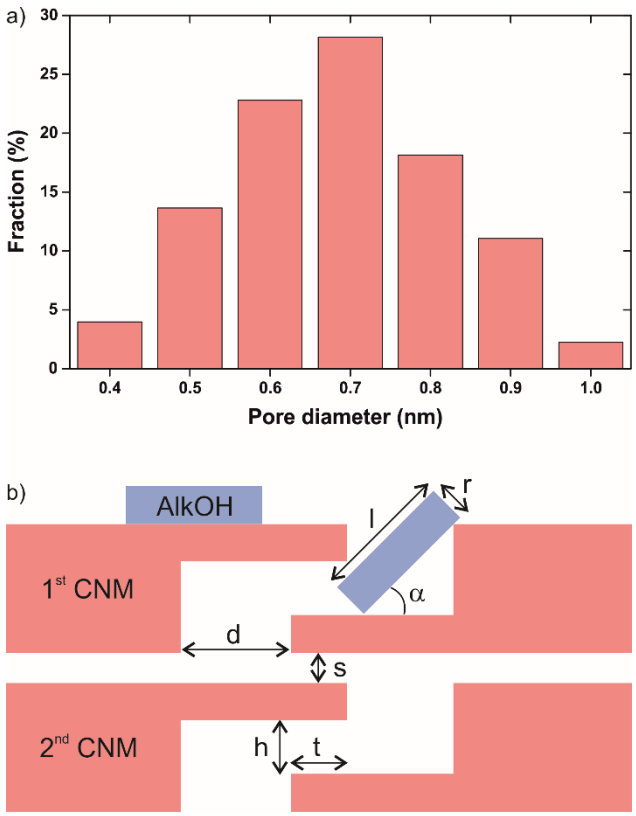

Figure 2. a) Size distribution of the CNMs' pore entrances as revealed by AFM.[10] b) Cross-sectional view of the laminar structural model for CNMs' conduits. *l* is the length of a rod-like molecule, *r* is the cylinder diameter, *d* is the outer pore diameter, *t* is the twist parameter, *h* is the interlaminar parameter, s is the interlayer parameter.

Clearly, alcohol molecules are not rigid rods, and their diffusion through nanomembranes is a complex process governed by multiple types of interactions. In particular, the permeation of PrOH and BuOH in single-layer CNMs was enhanced upon mixing with saturated water vapor, similar to our previous studies with atmospheric gases.[17] It is evident that water molecules impose a kinetic control on the hydrophilic species, and the transport mechanism is solvent-assisted as opposed to the individual motion of the dry alcohols. The dissolved molecules are swept across the membrane with the flow of liquefied water, while self-diffusion governs the permeation of organic adsorbates. Unfortunately, systematic comparison of the 1-alkanols is not possible by such experiments because of the great differences in their saturation vapor pressures spanning more than a hundred of mbar (Fig. 1). To further examine the effect of the stacking on CNMs' separation performance, we designed a synthetic azeotrope, consisting of 60 mol% D_2O and 40 mol% PrOH (Fig. 3a). Since saturated heavy water and PrOH have almost identical pressure at room temperature, this model system can be conveniently prepared in the liquid phase prior to permeation measurements. After releasing to the gas phase, a homogeneous vaporous mixture of known content is immediately supplied to the sample. As illustrated in Fig. 3b, single-layer CNMs are able to separate the azeotrope, and the cross-membrane flux of water molecules remains as high as for water alone. Extrapolating to larger areas, the transport rate measured would correspond to a record value of 35 kg m^{-2} h^{-1}. Although the selectivity is only 330, the mass flow characteristic outperforms much that of the state-of-the-art zeolitic membranes.[5]

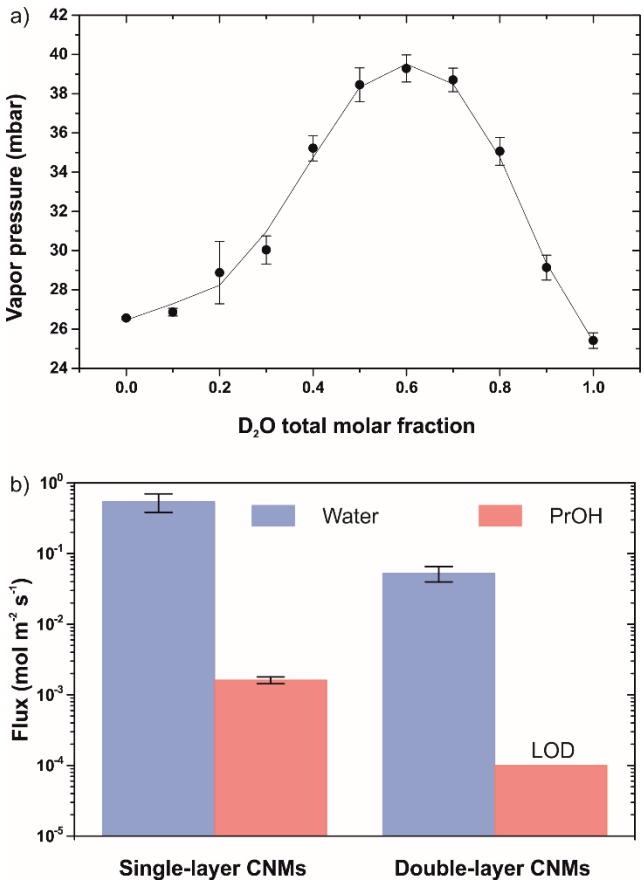

Figure 3. a) Saturation vapor pressure in D_2O/PrOH mixtures at room temperature (see supporting information for details). The data points are mean values over 3 measurements, and the error bars are standard deviation. The solid line is for guiding the eye. b) Transmembrane flux of D_2O and PrOH in single- and double-layer CNMs upon exposure to the vapor mixture of azeotropic composition. The data were averaged over 3-4 samples, and the error bars are standard deviation. LOD is the limit of detection as specified in ref. 18.

The double-layer CNMs demonstrated significantly improved water-alcohol separation, entirely retaining PrOH molecules (Fig. 3b). It is clear that the tight spacing between the layers is again responsible for the molecular sieving, but the most striking finding is that the flux of water was also suppressed. The tenfold decrease in the water permeation rate cannot be interpreted in light

of the interlayer bottleneck, because the transport of pure water in the CNMs stacks maintains its high rate and essentially appears similar to that in the single-layer membranes (Fig. 4a). Particularly, the flux of D_2O molecules in the double-layer membranes grows rapidly as the relative humidity increases and reaches its maximum upon saturation. As manifested earlier, water permeation in the nanomembranes is correlated with its adsorption isotherm, and the steep pressure dependence is described by the transition from the individual molecular passage to the cooperative flow of a liquid-like matter. Apparently, the single-file water motion is preserved in the double-layer CNMs as depicted schematically in Fig. 4b. The fact that water in the mixtures with PrOH does not experience any changes in the single-layer samples suggests that the model system behaves as a real azeotrope, and there is massive condensation occurring upon saturation. Now, to rationalize the observed slowdown effect, we recall that PrOH molecules do pass the single-layer CNMs along with water, whereas no flux is detected in the stacks under the same conditions. Our hypothesis is that the alcohol crosses the first layer and gets stuck in the interlayer spacing (Fig. 4b). The diffusion barrier increases the concentration of organic molecules between the layers and thus gives rise to the disruption of the single-file water. This can be considered as a "molecular jam" in nanoscale ducts and resembles the recent findings of Shin et al. who studied water/EtOH separation with GO membranes and observed a manifold decrease in the total transmembrane flux upon increasing the alcohol content in the feed mixture.[24] The authors performed molecular dynamics simulations and revealed formation of a blocking layer at the entrance to GO nanocapillaries. The mixture composition was also predicted to affect hydrocarbon/water transport in shale nanochannels, though for a much greater size scale.[25] It is remarkable that the process found in CNMs agrees well with the previously developed two-step kinetic model:[18]

$$F = k_{mono}\theta_{mono}n_0 + k_{multi}\theta_{multi}n_0$$

where F defines the transmembrane flux of water molecules, k_{mono} and k_{multi} stand for the rate constants of individual and collective transport, θ_{mono} and θ_{multi} are monolayer and multilayer coverage, respectively. As the "molecular jam" effectively switches off the single-file contribution ($k_{multi} \rightarrow 0$), the total flux is determined only by the individual-diffusion term ($k_{mono}\theta_{mono}n_0$). Given the saturation conditions, the apparent coverage θ_{mono} equals to 1. Using the same simulation parameters as before, one obtains 0.04 mol m^{-2} s^{-1} for the flux which is within the error consistent with our experiments (Fig. 3b).

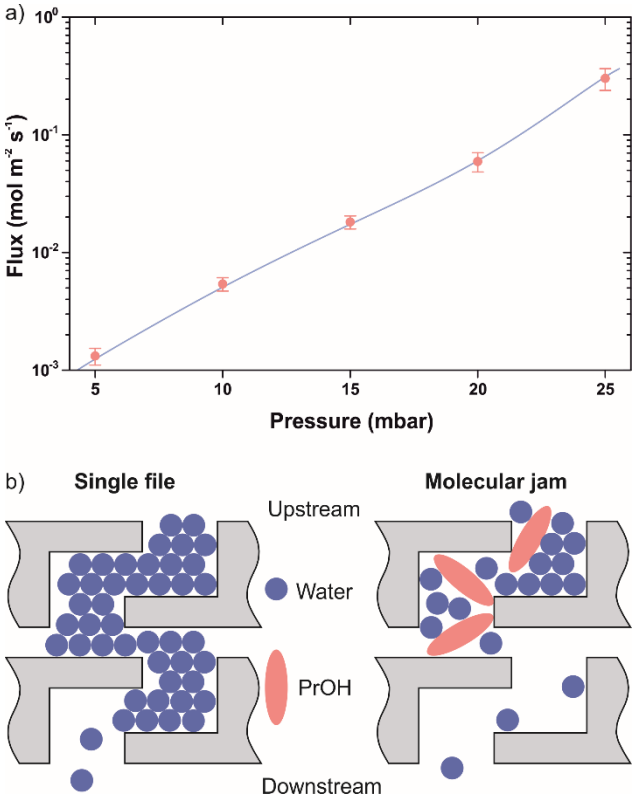

Figure 4. a) Transmembrane flux of D_2O in double-layer CNMs as a function of the feed pressure. The data points are mean values over three samples, and the error bars are standard deviation. 25 mbar is the saturation vapor pressure of D_2O at room temperature. The solid line is solely for guiding the eye. b) Schematic representation of the single-file and disrupted permeation mechanisms of water in the stacked CNMs.

To summarize, we for the first time studied molecular permeation in free-standing bilayer CNMs. The internal structure of the membranes was examined in an elegant manner by measuring transport rates of homologous 1-alkanols. The results revealed that interlayer spacing in the CNM stacks is much narrower than their intrinsic channels. Moreover, the nanomembranes were confirmed to be suitable for dehydration of azeotropic mixtures, and future work will focus on improving their performance both in terms of selectivity and throughput. Multilayer stacking was proven to be a promising approach, albeit its practical meaning is under question. We also observed the effect of a "molecular jam" in nanochannels which is nothing else than concentration polarization in vapor permeation. The single-file water motion was demonstrated to be broken down by bulky organic solutes, and the experimental findings matched well the kinetic interpretation. Experiments with variable vapor composition are needed to shed more light on the impact of concentration on molecular diffusion in nanoscale pores. This work highlights the ACP approach as a method for exploring functional interfaces.

EXPERIMENTAL METHODS

In this work, we used the same type of CNMs as in the previous studies.[10,17,18] The material was prepared by electron irradiation of [1",4',1',1]-Terphenyl-4-thiol (TPT, Sigma-Aldrich) monolayers on Au(111)/mica substrates (G. Albert PVD, Germany).[23] For permeation experiments, the CNMs were transferred from the Au substrate onto Si_3N_4/Si chips with around 7 μm sized circular orifices in Si_3N_4 membrane windows (Silson Ltd, UK). The transfer process was achieved with the assistance of PMMA protecting layers. Double-layer CNMs were prepared by placing a single-layer CNM with PMMA coatings on top of another CNM on Au substrate.[19] Then,

this stack was transferred onto silicon chips. The final step was the removal of PMMA layers by acetone.

The permeation measurements were conducted in the experimental system detailed elsewhere.[18] Briefly, suspended CNM samples were secured between a high-vacuum detection chamber with a quadrupole mass-spectrometer and a multi-section feed compartment. All experiments were carried out at room temperature. Heavy water (Sigma-Aldrich, 99.9% atom D), methanol (VWR Chemicals, 100%), ethanol (VWR Chemicals, 99.93%), 1-propanol (Chem Solute, > 99.5%), 1-butanol (AppliChem Panreac, 99.5%) were thoroughly outgassed before use. Please refer to the supporting information for the preparation of the model azeotropic mixture.

AUTHOR INFORMATION

Corresponding Authors

*E-mail: dementyev@physik.uni-bielefeld.de (P. D)

*E-mail: yang.yang1@imperial.ac.uk (Y.Y.)

Notes

The authors declare the following possible conflicts of interest: A. G. is a co-founder and shareholder of CNM Technologies GmbH, a company that specializes on the development of carbon nanomembranes. Y. Y. and A. G. are co-authors of a patent for A Method for Separating Fluidic Water from Impure Fluids and a Filter, which is related to the published research.

ACKNOWLEDGMENT

P. D. acknowledges financial support from the “Fonds der Chemischen Industrie” (Liebig Fellowship) and the Max-Buchner-Forschungsstiftung (Max-Buchner Fellowship). Y. Y. acknowledges the funding from the European Union’s Horizon 2020 research and innovation

program under the Marie Sklodowska-Curie grant agreement No. 838593. M. R. is grateful to the German Academic Exchange Service (DAAD) for a Research Fellowship (Grant No. 57440917). The authors also thank the German Federal Ministry for Education and Research (BMBF) (Grants No. 03XP0155A and 02WIL1453B).

SUPPORTING INFORMATION AVAILABLE

Experimental and theoretical details on preparation of the model heavy water-propanol azeotropic mixture for ACP measurements.

REFERENCES

(1) Climate Change and Land: an IPCC special report on climate change, desertification, land degradation, sustainable land management, food security, and greenhouse gas fluxes in terrestrial ecosystems (SRCCL). Intergovernmental Panel on Climate Change, 2019. https://www.ipcc.ch/srccl-report-download-page/ (Access date December 14, 2019)

(2) Vane, L. M. Separation Technologies for the Recovery and Dehydration of Alcohols from Fermentation Broths. *Biofuels, Bioprod. Bioref.* **2008**, *2*, 553-588.

(3) Huang, Y.; Ly, J.; Nguyen, D.; Baker, R. W. Ethanol Dehydration Using Hydrophobic and Hydrophilic Polymer Membranes. *Ind. Eng. Chem. Res.* **2010,** *49,* 12067-12073.

(4) Smuleac, V.; Wu, J.; Nemser, S.; Majumdar, S.; Bhattacharyya, D. Novel Perfluorinated Polymer-Based Pervaporation Membranes for the Separation of Solvent/Water Mixtures. *J. Membr. Sci*. **2010**, *352*, 41-49.

(5) Gao, X.; Zou, X.; Zhang, F.; Zhang, S.; Ma, H.; Zhao, N.; Zhu, G. Eco-friendly Fabrication of Hydrophilic ZSM-5 Membranes for Alcohol Upgrading. *Chem. Commun.* **2013**, *49*, 8839-8841.

(6) Nair, R. R.; Wu, H. A.; Jayaram, P. N.; Grigorieva, I. V.; Geim, A. K. Unimpeded Permeation of Water Through Helium-Leak-Tight Graphene-Based Membranes. *Science* **2012**, *335*, 442-444.

(7) Ren, C.E.; Hatzell, K. B.; Alhabeb, M.; Ling, Z.; Mahmoud, K.A.; Gogotsi, Y. Charge- and Size-Selective Ion Sieving Through $Ti_3C_2T_x$ MXene Membranes. *J. Phys. Chem. Lett.* **2015**, *6*, 4026-4031.

(8) Holt, J. K.; Park, H. G.; Wang, Y.; Stadermann, M.; Artyukhin, A. B.; Grigoropoulos, C. P.; Noy, A.; Bakajin, O. Fast Mass Transport Through Sub-2-Nanometer Carbon Nanotubes. *Science* **2006**, *312*, 1034-1037.

(9) Surwade, S. P.; Smirnov, S. N.; Vlassiouk, I. V.; Unocic, R. R.; Veith, G. M.; Dai, S.; Mahurin, S. M. Water Desalination Using Nanoporous Single-Layer Graphene. *Nature Nanotech.* **2015**, *10*, 459-464.

(10) Yang, Y.; Dementyev, P.; Biere, N.; Emmrich, D.; Stohmann, P.; Korzetz, R.; Zhang, X.; Beyer, A.; Koch, S.; Anselmetti, D.; *et al*. A. Rapid Water Permeation through Carbon Nanomembranes with Sub-Nanometer Channels. *ACS Nano* **2018**, *12*, 4695-4701.

(11) Reiter, G. F.; Deb, A.; Sakurai, Y.; Itou, M.; Kolesnikov, A. I. Quantum Coherence and Temperature Dependence of the Anomalous State of Nanoconfined Water in Carbon Nanotubes. *J. Phys. Chem. Lett.* **2016**, *7*, 4433-4437.

(12) Tunuguntla, R. H.; Henley, R. Y.; Yao, Y.-C.; Pham, T. A.; Wanunu, M.; Noy, A. Enhanced Water Permeability and Tunable Ion Selectivity in Subnanometer Carbon Nanotube Porins. *Science* **2017**, *357*, 792-796.

(13) Garnier, L.; Szymczyk, A.; Malfreyt, P.; Ghoufi, A. Physics behind Water Transport through Nanoporous Boron Nitride and Graphene. *J. Phys. Chem. Lett*. **2016**, *7*, 3371-3376.

(14) Hassan, J.; Diamantopoulos, G.; Gkoura, L.; Karagianni, M.; Alhassan, S.; Kumar, S. V.; Katsiotis, M. S.; Karagiannis, T.; Fardis, M.; Panopoulos, N.; *et al*. Ultrafast Stratified Diffusion of Water Inside Carbon Nanotubes; Direct Experimental Evidence with 2D $D-T_2$ NMR Spectroscopy. *J. Phys. Chem. C.* **2018**, *122*, 10600-10606.

(15) Ruiz-Barragan, S.; Muñoz-Santiburcio, D.; Marx, D. Nanoconfined Water within Graphene Slit Pores Adopts Distinct Confinement-Dependent Regimes. *J. Phys. Chem. Lett*. **2019**, *10*, 329-334.

(16) Schrier, J. Carbon Dioxide Separation with a Two-Dimensional Polymer Membrane. *ACS Appl. Mater. Interfaces* **2012**, *4*, 3745-3752.

(17) Naberezhnyi, D.; Gölzhäuser A.; Dementyev, P. Water-Assisted Permeation of Gases in Carbon Nanomembranes. *J. Phys. Chem. Lett*. **2019**, *10*, 5598-5601.

(18) Dementyev, P.; Wilke, T.; Naberezhnyi, D.; Emmrich, D.; Gölzhäuser, A. Vapour Permeation Measurements with Free-Standing Nanomembranes. *Phys. Chem. Chem. Phys.* **2019**, *21*, 15471-15477.

(19) Ai, M.; Shishatskiy, S.; Wind, J.; Zhang, X.; Nottbohm, C. T.; Mellech, N.; Winter, A.; Vieker, H.; Qiu, J.; Dietz, K.-J.; Gölzhäuser, A.; *et al*. Carbon Nanomembranes (CNMs) Supported by Polymer: Mechanics and Gas Permeation. *Adv. Mater*. **2014**, *26*, 3421-3426.

(20) Matei, D. G.; Weber, N.-E.; Kurasch, S.; Wundrack, S.; Woszczyna, M.; Grothe, M.; Weimann, T.; Ahlers, F.; Stosch, R.; Kaiser, U.; *et al*. A. Functional Single-Layer Graphene Sheets from Aromatic Monolayers. *Adv. Mater.* **2013**, *25*, 4146-4151.

(21) Marcus, Y. The Sizes of Molecules – Revisited. *J. Phys. Org. Chem.* **2003**¸*16*, 398-408.

(22) Androulidakis, C.; Zhang, K.; Robertson, M.; Tawfick, S. Tailoring the Mechanical Properties of 2D Materials and Heterostructures. *2D Mater*. **2018**, *5*, 032005.

(23) Angelova, P.; Vieker, H.; Weber, N.-E.; Matei, D.; Reimer, O.; Meier, I.; Kurasch, S.; Biskupek, J.; Lorbach, D.; Wunderlich, K.; *et al*. A Universal Scheme to Convert Aromatic Molecular Monolayers into Functional Carbon Nanomembranes. *ACS Nano* **2013**, *7*, 6489-6497.

(24) Shin, Y.; Taufique, M. F. N.; Devanathan, R.; Cutsforth, E. C.; Lee, J.; Liu, W.; Fifield, L. S.; Gotthold, D. W. Highly Selective Supported Graphene Oxide Membranes for Water-Ethanol Separation. *Sci. Rep.* **2019**, *9*, 2251.

(25) Li, Z.; Yao, J.; Kou, J. Mixture Composition Effect on Hydrocarbon-Water Transport in Shale Organic Nanochannels. *J. Phys. Chem. Lett*. **2019**, *10*, 4291-4296.